

Supporting Information

Perfluorinated Organics Regulating Li₂O₂ Formation and Improving Stability for Li–Oxygen Batteries

Yuling Wang,^{ab} Fan Bai,^b Aiping Wang,^a Zhonghui Cui,^b Da Wang,^{*a} Siqi Shi,^a Tao Zhang^{*b}

Abstract: Lithium-oxygen batteries have a high theoretical capacity, but they are still far from that value in practical applications. In this study, we systematically investigate the synergistic effect of perfluorotributylamine (PFTBA) as an additive in TEGDME-based electrolyte to optimize the electrochemical performance of Li-O₂ batteries. PFTBA promotes the growth of cyclic Li₂O₂, and the discharge capacity is increased to 9548.7 mAh·g⁻¹. The hydrophobicity PFTBA can protect lithium anode against corrosion while itself remains stable during cycling. The Li-O₂ battery was consequently possessed of enhanced cycling stability (200 cycles). This study reveals that the contribution of PFTBA in increasing the capacity and provides more possibilities for the application of perfluorinated chemicals in Li-O₂ batteries in the future.

^a School of Material Science & Engineering, Shanghai University, Shanghai 200072, P.R. China

*Corresponding Author: E-mail: dwd0826@shu.edu.cn

^b The State Key Lab of High Performance Ceramics and Superfine microstructure, Shanghai Institute of Ceramics, Chinese Academy of Sciences, 1295 Dingxi Road, Shanghai, 200050, P. R. China.

*Corresponding Author: E-mail: taozhang@mail.sic.ac.cn

DOI: 10.1039/x0xx000

Experimental Section

Preparation of electrolyte and electrodes

TEGDME was purchased from Aladdin and is further dried over 4Å molecular sieves in an argon filled glove box (O_2 and $H_2O < 0.1\text{ppm}$). LiTFSI from Aladdin was vacuum dried at 80°C for 12h. PFTBA was purchased from Aladdin. A TEGDME-based electrolyte consisted of Li salt of 1M lithium bis(trifluoromethane sulfonyl)imide (LiTFSI). The different content of PFTBA was added to TEGDME-based electrolyte and then was dispersed by ultrasonic oscillations after 2h, and the electrolyte with PFTBA could keep even for more than 1 month. The cathodes were prepared by mixing Multi-wall carbon nanotubes (MWCNTs, XFNANO, 8-15nm) and polyvinylidene fluoride (PVDF) with the weight ratio of 9:1 and stir to a homogenous slurry with N-methyl-2-pyrrolidone. Then the slurry was coated onto carbon paper, and vacuum dried at 80°C for 24h. The loading weight of MWCNT was ≈ 0.15 mg. The Li foil with a thickness of 0.2mm was cut into a disc with a diameter of 12.0mm, then pressed onto a stainless steel spacer in Li-O₂ batteries.

Assembling Li-O₂ coin cell

Cells were assembled in an Ar filled glove box (O_2 and $H_2O < 0.1\text{ppm}$). A Li-O₂ cell consists of the MWCNT cathode, the lithium metal anode and a Waterman GF/C glass fiber between cathode and anode with 80 μL electrolyte.

Calculation Details

The Highest Unoccupied Molecular Orbital (HOMO) of TEGDME and PFTBA were obtained at the B3LYP/6-311g* level with the Gaussian 09^[1].

Material characterization and Electrochemical analysis

The mixed solution of TEGDME with different content of PFTBA was prepared in the bottles, and then place the bottles in a container with good airtightness. The above

preparations are operated in the glove box with Ar. Then let O₂ continuously into the glass bottle filled with the solution. And then use the dissolved oxygen meter to test the oxygen solubility of the solution after 12h. X-ray diffraction (BRUKER AXS GMBH (D8 ADVANCE)) was used to analyze the discharge products on the cathode of Li-O₂ cells with Cu K α radiation at the angle range of 10-80°. The observation of cathodes was analyzed by scanning electron microscope (FE-SEM, SU8220). The samples were removed from cells after cycling in argon-filled glove box, and the cathodes obtained were washed with 1,2-dimethoxyethane (anhydrous, Sigma) and then dried for 2h. And then the samples were sealed in an aluminum foil bag to avoid the air. The Li anodes and cathodes removed from cells after cycling were washed with 1,2-dimethoxyethane and detected by the X-ray photoelectron spectroscopy (XPS, Thermo Fisher Scientific ESCALAB 250). The Li anodes after cycling were analyzed by Fourier transform infrared (FTIR, JASCO FT/IR-6200).

Table

Electrolytes	0mM PFTBA	100mM PFTBA	300mM PFTBA
Ionic conductivity (S/cm)	1.18×10^{-2}	1.07×10^{-2}	9.76×10^{-3}

Table 1 The ionic conductivity of the TEGDME-based electrolyte with different content of PFTBA

Figures

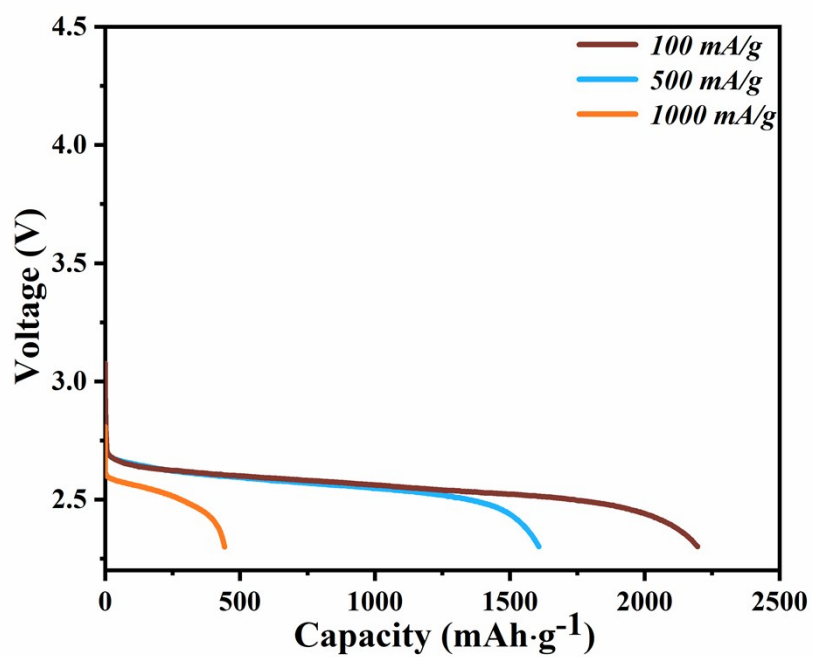


Fig.S1 Discharge profiles of Li-O₂ batteries with TEGDME-based electrolyte under various current density

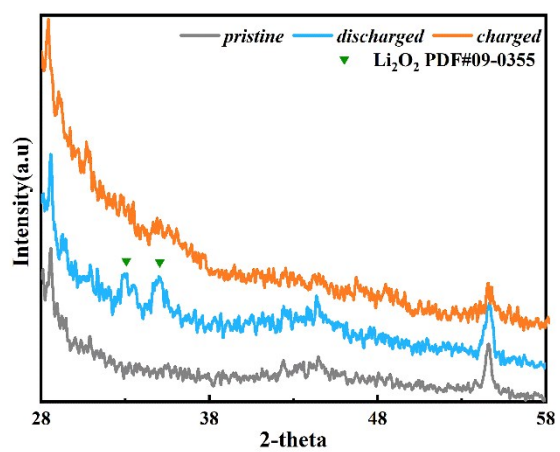


Fig.S2 XRD pattern of the cathodes in Li-O₂ cells with PFTBA additives.

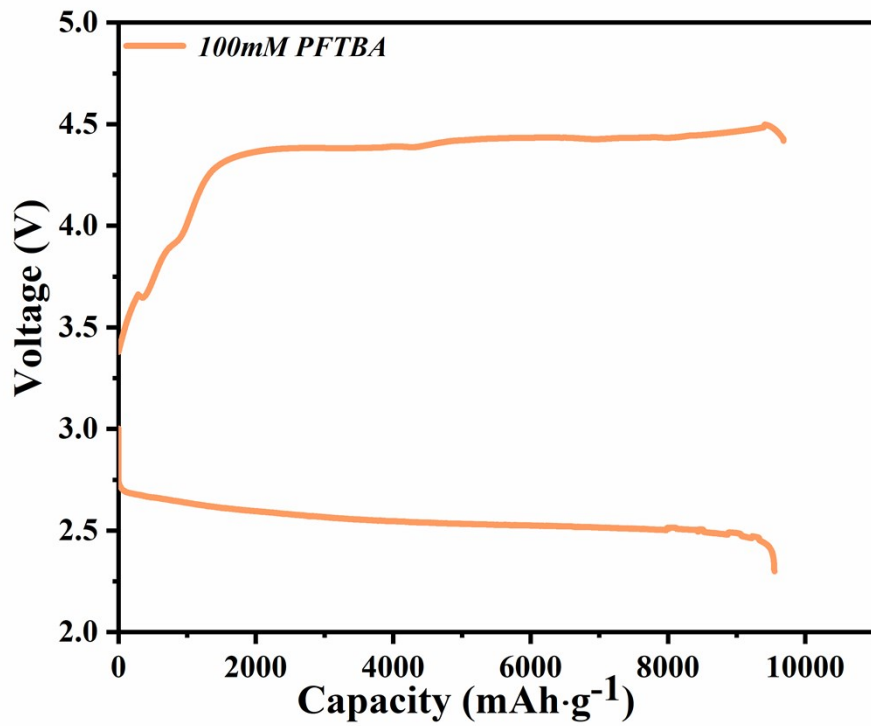


Fig.S3 Full discharge/charge profile of Li-O₂ battery with 100mM PFTBA at 500 mA g⁻¹.

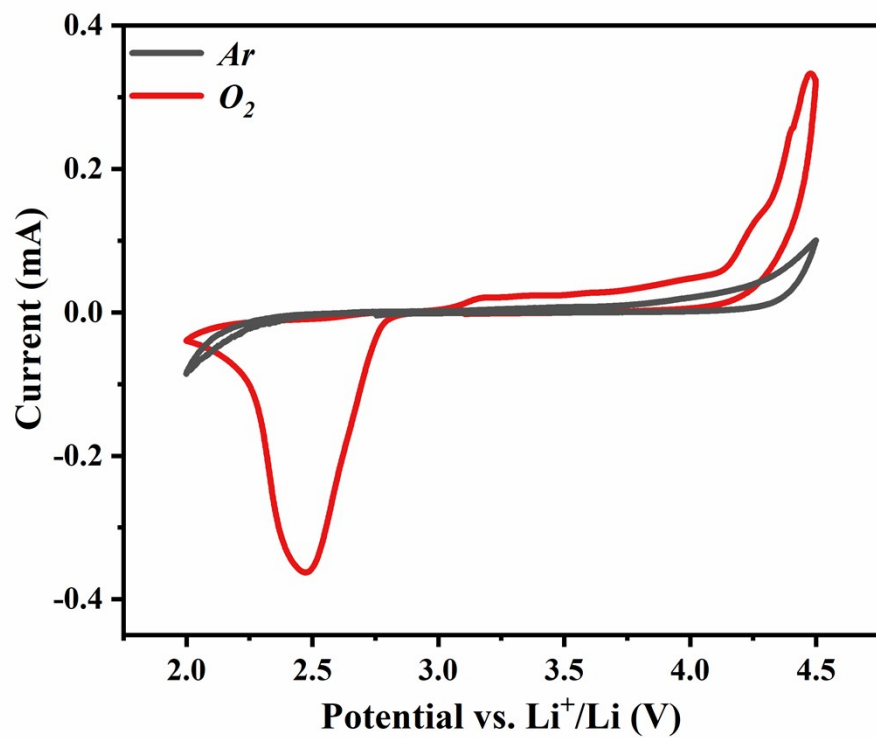


Fig. S4 Cyclic voltammograms of Li-O₂ cells with PFTBA in Ar and O₂.

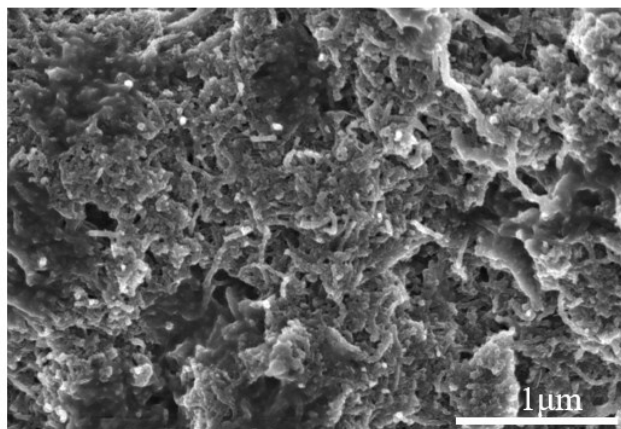


Fig. S5 SEM image of discharged air cathode from the TEGDME-based battery without PFTBA.

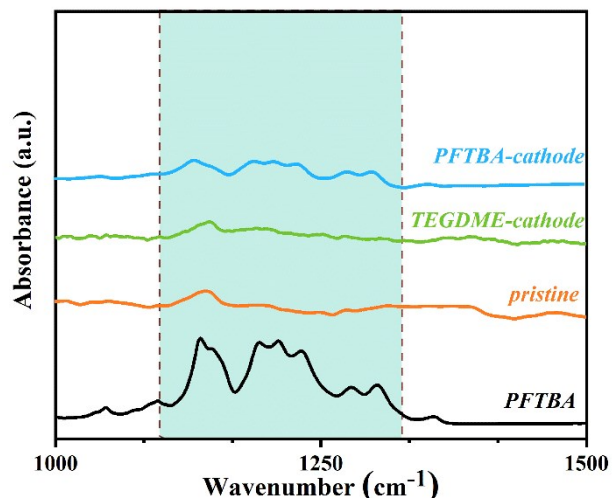


Fig.S6 FTIR of the cathodes soaked in TEGDME solutions with and without PFTBA

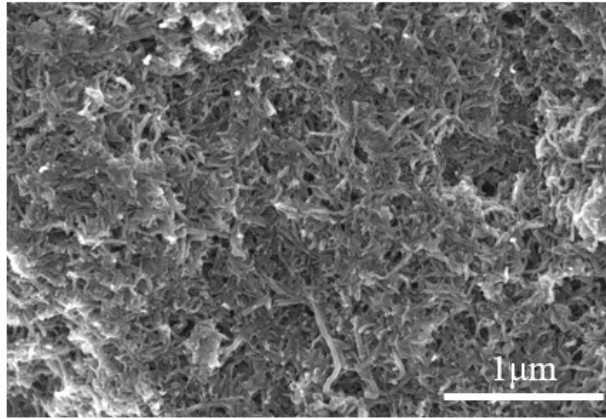


Fig.S7 SEM of the air cathode of the Li-O₂ battery with 100mM PFTBA after 40 cycles.

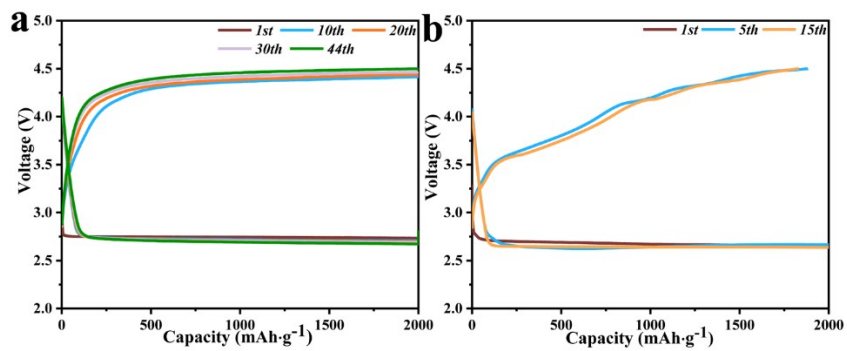


Fig.S8 Electrochemical performance of Li-O₂ cells with PFTBA (a) and (b) without PFTBA.

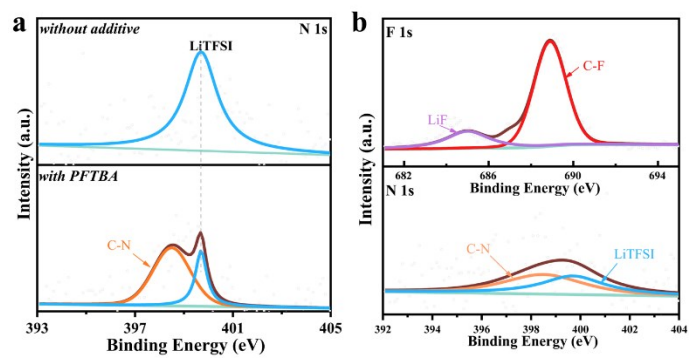


Fig.S9 XPS spectra of the cathodes in Li-O₂ cells with PFTBA after 20cycles (a) and 40 cycles (b).

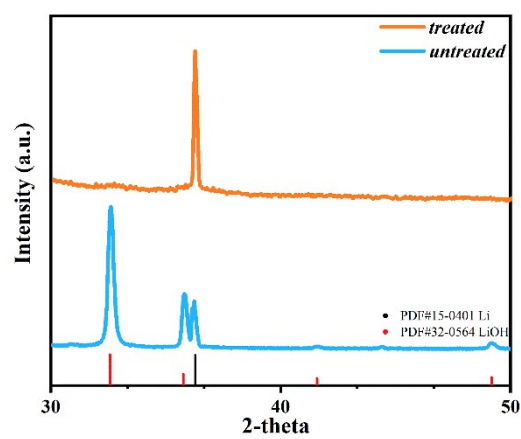


Fig.S10 XRD pattern of the treated and untreated Li foils exposed to air after 5 min

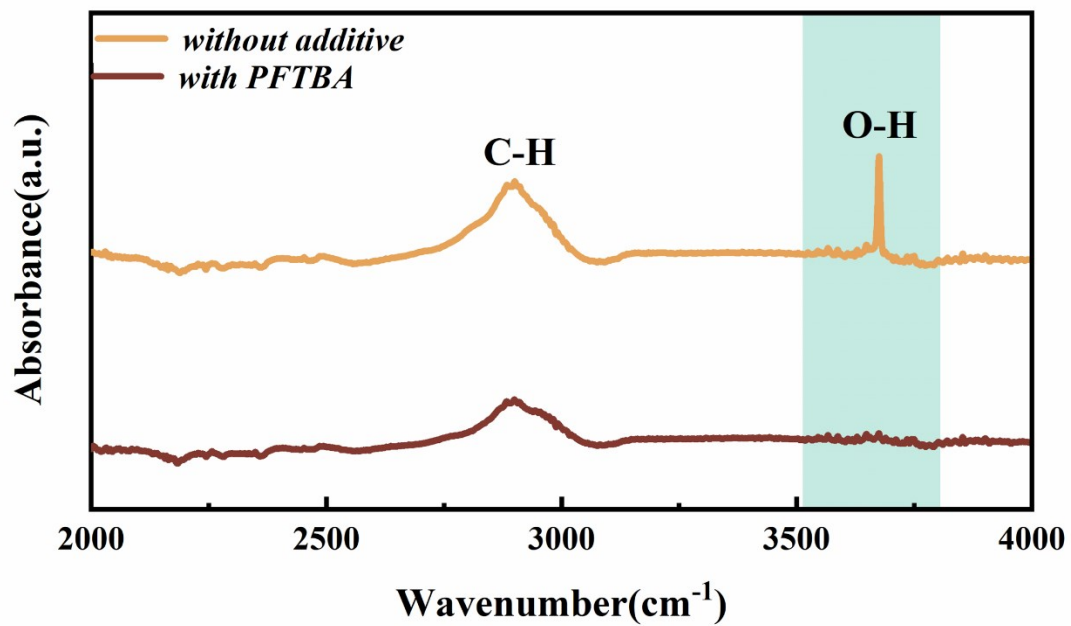


Fig.S11 FTIR spectra on the surface of Li anodes with or without PFTBA after 40 cycles.

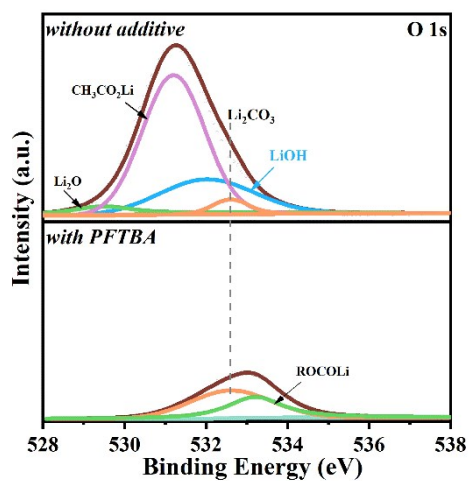


Fig.S12 XPS spectra of the Li anodes in Li-O₂ cells with and without PFTBA after 20 cycles.

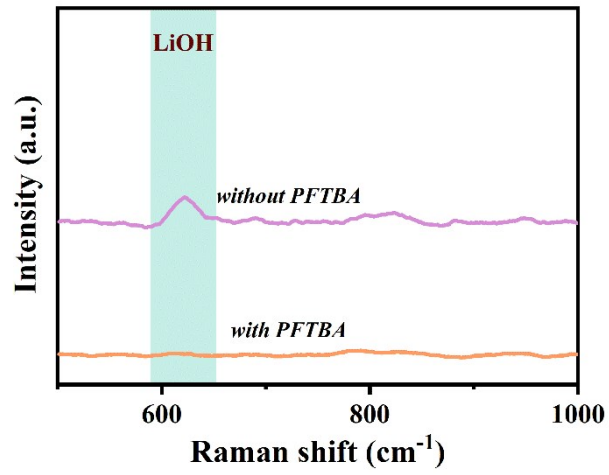


Fig.S13 Raman spectra of the cathodes in Li-O₂ cells with and without PFTBA after 20 cycles.

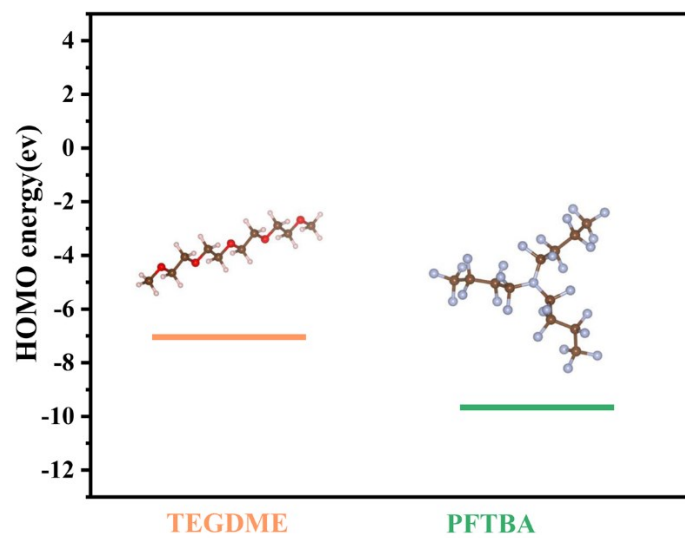


Fig.S14 HOMO energy of TEGDME and PFTBA. The brown, pink, red, and purple balls respectively represent C atom, H atom, O atom and F atom.

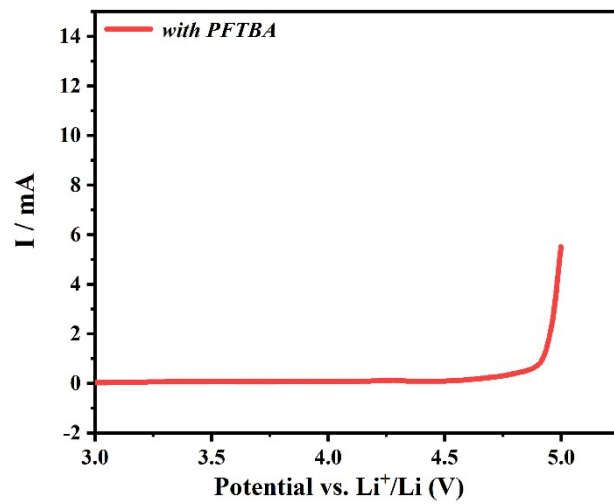


Fig.S15 LSV curve of the electrolyte with 100mM PFTBA.

Reference

[1] Frisch, M. J., G. W. Trucks, H. B. Schlegel, G. E. Scuseria, M. A. Robb, J. R. Cheeseman, G. Scalmani, V. Barone, G. A. Petersson, H. Nakatsuji, X. Li, M. Caricato, A. V. Marenich, J. Bloino, B. G. Janesko, R. Gomperts, B. Mennucci, H. P. Hratchian, J. V. Ortiz, A. F. Izmaylov, J. L. Sonnenberg, Williams, F. Ding, F. Lipparini, F. Egidi, J. Goings, B. Peng, A. Petrone, T. Henderson, D. Ranasinghe, V. G. Zakrzewski, J. Gao, N. Rega, G. Zheng, W. Liang, M. Hada, M. Ehara, K. Toyota, R. Fukuda, J. Hasegawa, M. Ishida, T. Nakajima, Y. Honda, O. Kitao, H. Nakai, T. Vreven, K. Throssell, J. A. Montgomery Jr., J. E. Peralta, F. Ogliaro, M. J. Bearpark, J. J. Heyd, E. N. Brothers, K. N. Kudin, V. N. Staroverov, T. A. Keith, R. Kobayashi, J. Normand, K. Raghavachari, A. P. Rendell, J. C. Burant, S. S. Iyengar, J. Tomasi, M. Cossi, J. M. Millam, M. Klene, C. Adamo, R. Cammi, J. W. Ochterski, R. L. Martin, K. Morokuma, O. Farkas, J. B. Foresman and D. J. Fox. Gaussian 09, Revision D.01. Wallingford, CT, 2013.